Joule

CellPress

Article

Continuous Carbon Dioxide Electroreduction to Concentrated Multi-carbon Products Using a Membrane Electrode Assembly

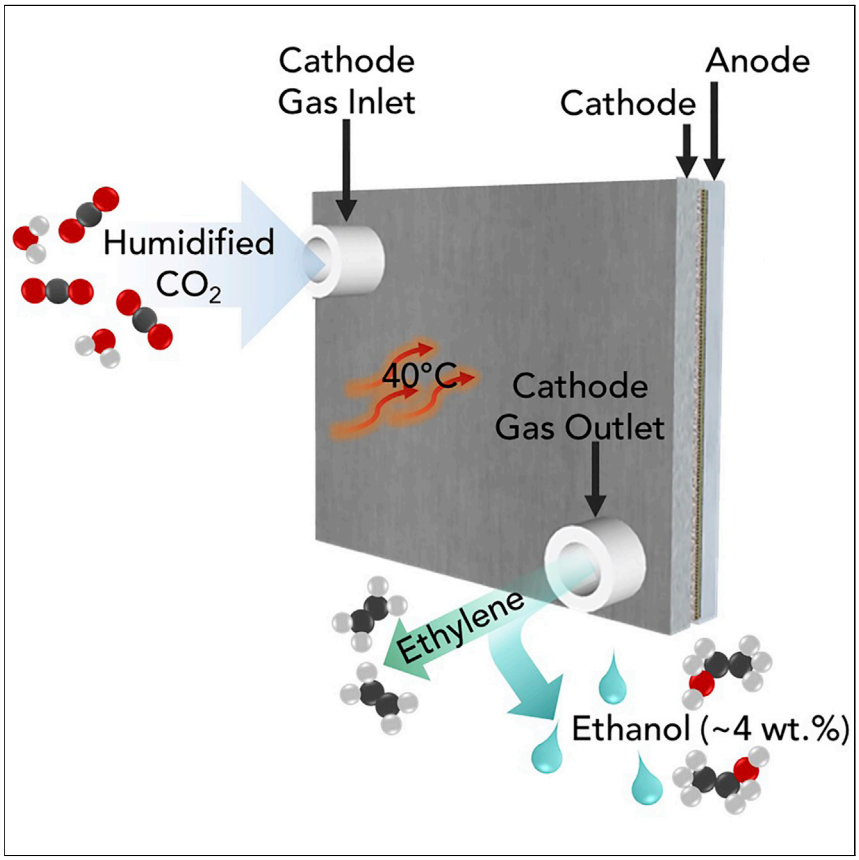

Electrochemical CO_2 reduction is a promising strategy to synthesize valuable multi-carbon products (C_{2+}) while sequestering CO_2 and utilizing intermittent renewable electricity. Here, we present a stable membrane electrode assembly (MEA) electrolyzer that converts CO_2 to C_{2+} products. This strategy achieves ~50% and ~80% selectivity for ethylene and C_{2+} products, respectively, with cathode outlet concentrations of ~30% ethylene and the direct production of ~4 wt % ethanol. We characterize stability by operating continuously for 100 h with steady ethylene production.

Christine M. Gabardo, Colin P. O'Brien, Jonathan P. Edwards, ..., Jun Li, Edward H. Sargent, David Sinton

sinton@mie.utoronto.ca

HIGHLIGHTS

Membrane electrode assembly design enables stable CO_2 electroreduction

~50% Faradaic efficiency for ethylene and ~80% Faradaic efficiency for C_{2+} products

>30% gas outlet concentration of ethylene and direct production of ~4 wt % ethanol

Continuous 100 h operation at >100 mA cm^{-2}

Gabardo et al., Joule 3, 1–15
November 20, 2019
https://doi.org/10.1016/j.joule.2019.07.021

Please cite this article in press as: Gabardo et al., Continuous Carbon Dioxide Electroreduction to Concentrated Multi-carbon Products Using a Membrane Electrode Assembly, Joule (2019), https://doi.org/10.1016/j.joule.2019.07.021

Joule

CellPress

Article

Continuous Carbon Dioxide Electroreduction to Concentrated Multi-carbon Products Using a Membrane Electrode Assembly

Christine M. Gabardo,[1,3] Colin P. O'Brien,[1,3] Jonathan P. Edwards,[1] Christopher McCallum,[1] Yi Xu,[1] Cao-Thang Dinh,[2] Jun Li,[1,2] Edward H. Sargent,[2] and David Sinton[1,4,*]

SUMMARY

Electrochemical carbon dioxide (CO_2) reduction is a promising strategy to synthesize valuable multi-carbon products (C_{2+}) while sequestering CO_2 and utilizing intermittent renewable electricity. For industrial deployment, CO_2 electrolyzers must remain stable while selectively producing concentrated C_{2+} products at high rates with modest cell voltages. Here, we present a membrane electrode assembly (MEA) electrolyzer that converts CO_2 to C_{2+} products. We perform side-by-side comparisons of state-of-the-art electrolyzer systems and find that the MEA provides the most stable cell voltage and product selectivity. We then demonstrate an approach to release concentrated gas and liquid products from the cathode outlet. This strategy achieves ~50% and ~80% Faradaic efficiency for ethylene and C_{2+} products, respectively, with cathode outlet concentrations of ~30% ethylene and the direct production of ~4 wt % ethanol. We characterize stability by operating continuously for 100 h, the longest stable ethylene production at current densities >100 mA cm^{-2} among reported CO_2 electrolyzers.

INTRODUCTION

Rising atmospheric CO_2 levels have motivated reduced fossil fuel usage and a transition toward less carbon-intensive technologies. The electrochemical reduction of CO_2 to fuels and chemical feedstocks has gained attention as a means to close the carbon cycle (fuels) or sequester CO_2 into chemical feedstocks for the materials industry (feedstocks), all powered using renewable energy.[1,2]

Of the possible chemicals generated through the electrochemical CO_2 reduction reaction (CO_2RR), those containing carbon-carbon bonds, such as ethylene and ethanol, are sought in view of their high-energy-density and market value. Many copper (Cu)-based catalysts have achieved high selectivity (Faradaic efficiency, FE) toward C_{2+} products during CO_2RR.[3] The overpotential has been lowered through catalyst tuning[3–5] and electrolyte engineering, also contributing to progress in electrochemical energy efficiency (EE), the product of voltage efficiency (VE), the ratio of thermodynamic cell potential to the applied cell potential), and FE.[6,7]

Techno-economic analysis highlights the importance of operating at high reaction rates: current densities above 100 mA cm^{-2}. These high rates are needed to ensure that the capital cost of the CO_2RR electrolyzer (amortized over its operating lifetime) makes an acceptably low contribution to the total chemical product cost.[8,9] Moreover, additional energy costs are incurred because of the downstream separation

Context & Scale

The advent of low-cost renewable electricity and rising atmospheric CO_2 has led to a focus on electrochemical CO_2 reduction as a means toward low-carbon-intensity fuels and chemical feedstocks. The conversion of CO_2 into C_{2+} hydrocarbons and oxygenates (i.e., products containing two or more carbon atoms) is attractive in light of large global market demand for these high-energy-density products. A limited number of prior studies have focused on performance in the reaction rate regime above 100 mA cm^{-2} generally viewed as necessary for industrial deployment. In these works, gas diffusion electrodes are used in liquid electrolyte electrochemical flow cells, which suffer in system stability and/or energy efficiency. We overcome this issue by developing a membrane electrode assembly-based electrolyzer. The combined catalyst and system strategy produces concentrated gas and liquid products and maintains performance during long-term (100 h) uninterrupted operation.

of the CO_2RR products from each other, unreacted CO_2, and/or the liquid electrolyte. Ultimately, these energy costs decrease the total EE in electrosynthesizing the desired product, which is obtained by multiplying together the electrochemical, separation, and balance of plant energy efficiencies. Generating more concentrated CO_2RR products can reduce the financial burden of the separation processes from both the output gas and liquid streams.[10] Electrolyzers have produced concentrated acetate (6.5 wt %) and formate (1.8 wt %) from carbon monoxide (CO) and CO_2 feedstocks, respectively.[11,12]

Only by introducing CO_2 in the gas phase are the mass transport rates associated with CO_2 diffusion in aqueous electrolyte overcome. Alkaline flow cells, in which an alkaline electrolyte (usually potassium hydroxide, KOH) is flowed past the cathodic gas diffusion electrode (GDE), have achieved high current density production of ethylene,[6,7,13–15] ethanol,[16] acetate,[17] and n-propanol[18–20] from CO_2 or CO feedstocks. Operation of CO_2RR electrolyzers in highly alkaline environments has shown increased conductivity across the flow cell and improved reaction kinetics compared to those with less alkaline electrolytes.[6,21] Although very high current densities and EEs can be achieved with alkaline flow cells; they suffer from carbonate salt formation from the undesirable consumption of CO_2 by the KOH electrolyte. Neutral electrolytes, such as K_2SO_4 or $KHCO_3$, can replace alkaline electrolytes, but these have so far been limited to low EEs due to high ohmic resistance and overpotentials.[22,23] Maintaining the catholyte stability remains as an especially difficult issue of the CO_2RR system. The electrolyte can be altered by the absorption of CO_2 and/or the reaction-driven pH,[24,25] leading to salt precipitation on the GDE and/or ion exchange membrane and can lead to conductivity decreases throughout the system, decreasing the full cell EE. Moreover, liquid products that are generated, like alcohols and oxygenates, are diluted into the large volume of electrolyte, increasing downstream separation costs. Thus, designing a CO_2RR electrolyzer that can overcome these limitations and that is resistant to these electrolyte fluctuations is critical to developing an industrially suitable system.

In the MEA system, the cathodic GDE is pressed up directly against the ion exchange membrane. By eliminating the catholyte, issues associated with the electrolyte ohmic losses, electrolyte consumption with CO_2, electrolyte impurities fouling the catalyst, and electrolyte flooding through the GDE can be eliminated. MEA electrolyzers have been used to produce C_{2+} products, but so far only at low current densities (<100 mA cm^{-2}) when CO_2 is used as feedstock[26–31] due to the use of proton exchange membranes which create an acidic catalyst environment, favoring the hydrogen evolution reaction (HER) over the generation of C_{2+} products. Moreover, the formation of large quantities of liquid products at high current densities blocks CO_2 diffusion through the commercial carbon paper-based GDEs, leading to increased HER over time. Developing strategies to overcome the limitations of previous MEA systems would enable the generation of C_{2+} products in a more energy-efficient and stable system.

Here, we investigate liquid electrolyte flow cell and MEA systems that generate C_{2+} products via CO_2RR. We design a MEA electrolyzer to overcome the low reaction rates of previous MEA systems through the generation of a locally basic reaction environment at the catalyst and the integration of a cathode GDE that remains robust against liquid accumulation. This MEA electrolyzer strategy outperforms all liquid electrolyte flow cells in terms of voltage stability and product stability and significantly outperforms the reaction rate and stability of previous MEA electrolyzers. Next, we explore operating parameters that impact the MEA gas and liquid

[1]Department of Mechanical and Industrial Engineering, University of Toronto, Toronto, ON M5S 3G8, Canada

[2]Department of Electrical and Computer Engineering, University of Toronto, Toronto, ON M5S 1A4, Canada

[3]These authors contributed equally

[4]Lead Contact

*Correspondence: sinton@mie.utoronto.ca

https://doi.org/10.1016/j.joule.2019.07.021

Please cite this article in press as: Gabardo et al., Continuous Carbon Dioxide Electroreduction to Concentrated Multi-carbon Products Using a Membrane Electrode Assembly, Joule (2019), https://doi.org/10.1016/j.joule.2019.07.021

product concentrations, such as low CO_2 flow rates and elevated temperatures. Subsequently, we design a cathodic Cu catalyst strategy to take advantage of the high concentration of CO_2 at the catalyst, uniquely enabled by the MEA system, to achieve a high FE toward ethylene (~50%), a high FE and EE toward C_{2+} products (~80% and 23%, respectively), and the generation of concentrated ethanol (3.9 wt %). Finally, we present the stable and continuous production of these C_{2+} products for over 100 h at more than 100 mA cm^{-2}.

RESULTS AND DISCUSSION

Comparison of CO_2RR Electrolyzer Architectures

Cathode GDEs were prepared by sputtering Cu onto hydrophobic porous polytetrafluoroethylene (PTFE) membranes[6] that were subsequently spray-coated with conductive layers of carbon black and graphite particles (scanning electron microscopy (SEM) images of the sputtered layer in Figures S1A and S1B and diagram of the cathode in Figure S2). Anodes for the oxygen evolution reaction (OER) were prepared by coating titanium supports with iridium oxide (IrO_2, 2 mg cm^{-2})[32] (SEM images of the anode in Figures S1C and S1D).

An anion exchange membrane (AEM) was used to separate the cathode and anode compartments of the cell (photographs in Figures S1E and S1F), each side with a 5 cm^2 serpentine flow field. As CO_2 travels through the flow field, it diffuses through the PTFE layer to reach the Cu catalyst layer at either the liquid catholyte or polymer electrolyte (AEM) interface for the liquid flow cells and MEA electrolyzer, respectively.

Three electrolyzer configurations were compared: an alkaline flow cell (1 M KOH catholyte and anolyte, Figure 1A), a neutral flow cell (0.5 M K_2SO_4 or 1 M $KHCO_3$ catholyte and anolyte, Figures 1A and S4, respectively), and a MEA electrolyzer (0.1 M $KHCO_3$ anolyte, Figures 1A and S2). An additional flow field was used as the catholyte flow channel to convert the MEA electrolyzer cell into the alkaline and neutral flow cells (Figure S3) and each 50 mL electrolyte was recirculated. Each electrolyzer architecture was operated under galvanostatic electrolysis for 2 h at 750 mA (150 mA cm^{-2}), with the non-iR corrected full cell voltage monitored continuously (Figure 1B) and the FE of gas products quantified every 20 min (Figure 1C).

The alkaline flow cell began operating at a full cell voltage of −3.25 V; however, the voltage increased over the 2-h test to above −4.20 V. The increase in voltage can be explained by the uptake of CO_2 into the KOH electrolyte producing bicarbonate and carbonate. Experimentally, this is observed as a decrease in the catholyte and anolyte pH values and conductivities (Table S1). Despite the voltage instability, the gas product selectivity remained relatively stable over the 2 h test, with a slight decrease in ethylene FE (46% to <40%) (Figure 1C).

The neutral flow cell with 0.5 M K_2SO_4 remained at a full cell voltage of ~−5.0 V throughout the experiment. The higher cell voltage was due to electrolyte ohmic losses of 0.5 M K_2SO_4 combined with decreased reaction kinetics in the lower alkalinity environment. The pH gradient that developed between the cathode and anode over the course of the reaction led to an increase in both the catholyte and anolyte conductivity (Table S1), which may have counteracted the pH gradient-induced polarization losses to lead to this relatively stable voltage. Moreover, throughout the experiment, the FE toward ethylene and CO decreased, while that of hydrogen and methane both increased. A similar trend was observed with 1 M $KHCO_3$ electrolyte (Figure S4): thus, even with buffering capacity, the neutral flow cell electrolyte

Please cite this article in press as: Gabardo et al., Continuous Carbon Dioxide Electroreduction to Concentrated Multi-carbon Products Using a Membrane Electrode Assembly, Joule (2019), https://doi.org/10.1016/j.joule.2019.07.021

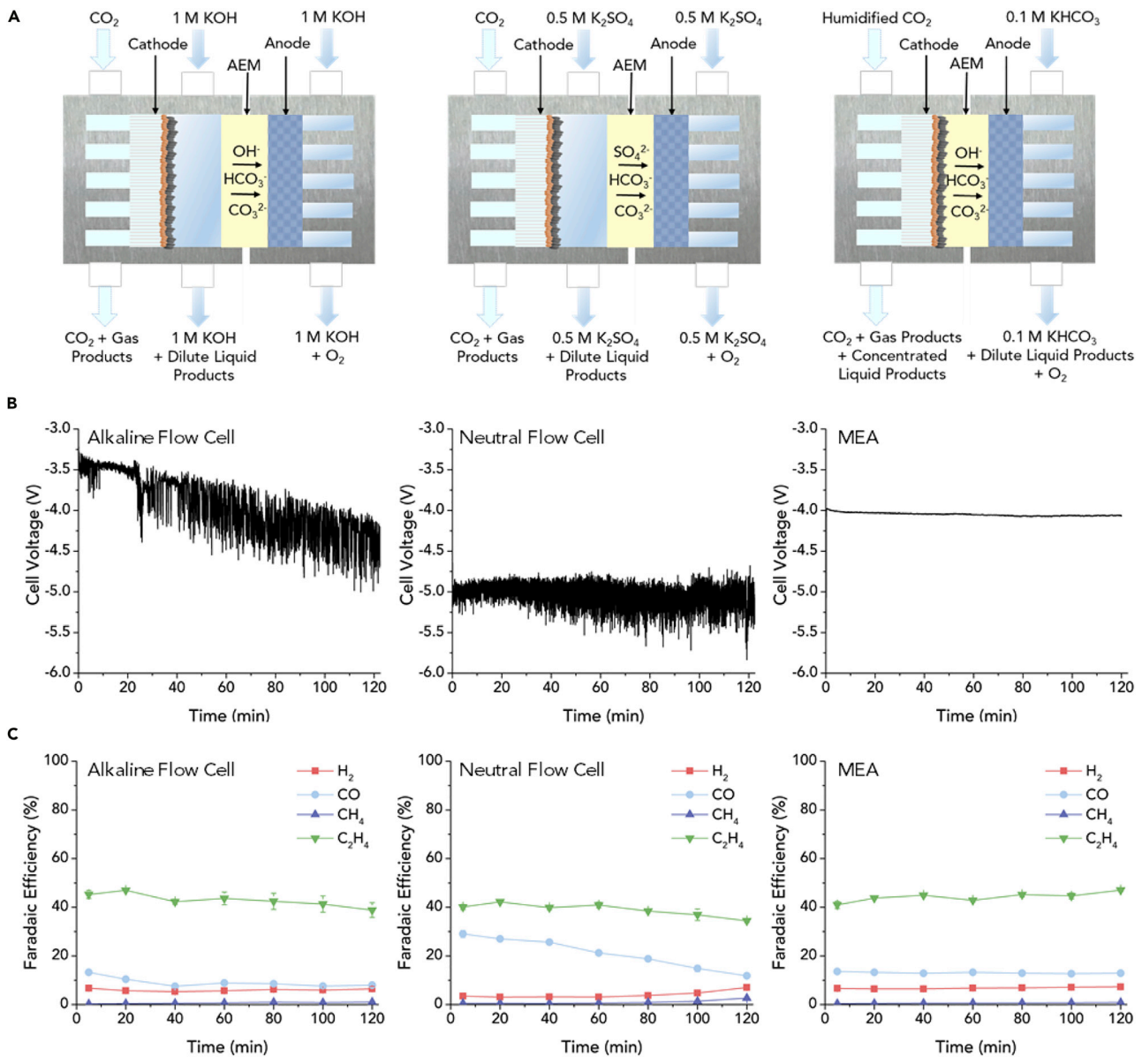

Figure 1. Voltage and Product Stability for Alkaline Flow Cell, Neutral Flow Cell, and Mea Electrolyzer

(A) Schematic of each cell configuration. The alkaline and neutral flow cells use 1 M KOH and 0.5 M K_2SO_4 for electrolytes in the cathode and anode compartments. The MEA cell uses 0.1 M $KHCO_3$ as electrolyte for the anode.

(B and C) Stability of the cell voltage (B) and gas products (C) for 120 min in each cell with an applied current of 750 mA (150 mA cm^{-2}). Error bars for gas products are calculated from the standard deviation of three samples taken at the same time.

environment and cell performance are unstable, an observation that could be explained through the precipitation of electrolyte salts in the system.[25]

We then turned to the realization of a catholyte-free MEA system employing an AEM along with a neutral anode electrolyte. Recent advances in AEM technology have led to membranes with lower resistances than previous generations that can be incorporated into MEAs to produce efficient electrolyzers.[33–35] We selected an AEM with the goal of generating a locally high pH at the catalyst by operating at a high current density. Locally high pH at the catalyst has been found to decrease the onset of

Please cite this article in press as: Gabardo et al., Continuous Carbon Dioxide Electroreduction to Concentrated Multi-carbon Products Using a Membrane Electrode Assembly, Joule (2019), https://doi.org/10.1016/j.joule.2019.07.021

CO production,[21] and thus promote C-C coupling when a sufficient surface coverage of this key intermediate for C_{2+} product generation is reached.[36,37] A carbon-based GDE was determined to be unsuitable for MEA integration because of the flooding of the electrode with water and liquid products during prolonged operation. This flooding decreased CO_2 diffusion to the catalyst, as evidenced by increased HER over time (Figure S5). We integrated our previously demonstrated[6] flooding-resistant PTFE GDE into our MEA system. The MEA electrolyzer (0.1 M $KHCO_3$ anolyte) maintained a stable voltage of −4 V, a much lower voltage than the 1 M $KHCO_3$ liquid flow cell. Increasing the concentration of the anolyte for the MEA has a slight benefit for the voltage but leads to less stable long-term operation.[38] The FE for ethylene increased from 43% to 47% over the 2 h operating time, while the HER FE remained constant, indicating that the PTFE GDE was more robust than the carbon-based GDE at expelling liquids and maintaining short CO_2 diffusion lengths through liquid. Measurements of anolyte pH and conductivity reveal that these were constant over the duration of the experiment to within 2% (Table S1).

The MEA electrolyzer provides the lowest stable voltage performance of the three electrolyzer architectures. It also provides the highest selectivity toward C_{2+} gas products. We therefore explored the influence of operating conditions and catalyst tuning on the performance of the MEA electrolyzer for concentrated C_{2+} chemical production.

Performance of the MEA Electrolyzer for Multi-carbon Product Generation

We characterized the current-voltage response of the MEA electrolyzer under ambient conditions (20°C, 1 atm) (Figure 2A). Between −2.8 and −4.2 V, the current density increased from 11 to over 200 mA cm^{-2}. For the gas products (Figure 2B), the CO selectivity decreased continuously with increasing cell voltage and current density. The FE for ethylene increased concurrently, reaching a maximum selectivity of nearly 50% FE at −4.1 V. The production of methane was negligible over all assessed voltages (<0.5% FE). The competing HER was decreased to below 5% FE at voltages more negative than −3 V.

The total gas FE decreased with increasing voltage, corresponding to a shift toward liquid products at higher voltages. We measured the selectivity for liquid products generated at the cathode by collecting from the cold trap connected to the cathode gas outlet and from the anolyte, to detect liquid products that may have crossed over the AEM with the flow of water and ions (Figure 2C). The production of ethanol and acetate increased as the voltage increased, reaching FEs of 15% and 7%, respectively. While most of the liquid products are detected in the anolyte (Figure S6A), a substantial quantity of the major liquid product, ethanol, was detected in the liquid collected from the cathode outlet at ~5% FE (0.5 wt %).

The total product FE was near 100%, indicating minimal oxidation of liquid products that travel to the anolyte (Figure S6B). In addition, a control experiment was conducted in which the liquid anolyte was spiked with typical concentrations of generated liquid products and was run for several hours under HER conditions at the cathode to avoid additional liquid product generation (150 mA cm^{-2}) (Figure S6C). Minimal loss in the spiked liquid products was observed, with the exception of formate, suggesting that most products that crossover the AEM to the anolyte are not oxidized. Iridium-based anode catalysts have shown activity for formic acid oxidation[39]; however, these catalysts show lower activity for alcohol oxidation.[40,41] The electromigration of acetate and formate across the AEM is expected because of their anionic charge, and formate was detected only in the anolyte (Figure S7); whereas the transport of the neutral alcohol products, ethanol and

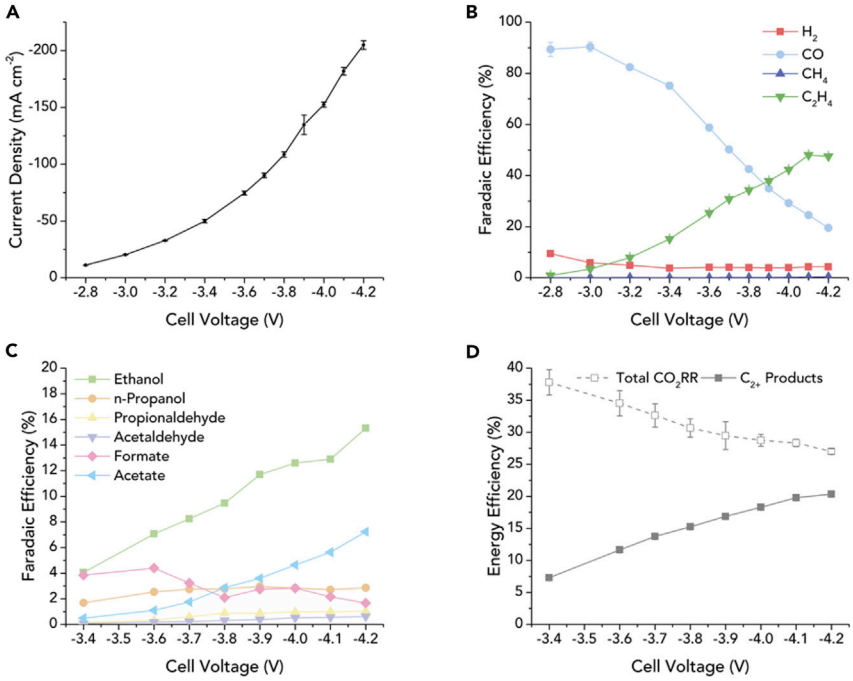

Figure 2. Electrocatalytic CO_2RR Performance of an MEA Electrolyzer

(A) Current and cell voltage relationship for the MEA electrolyzer. Error bars represent the standard deviation of the current density during the entire operation at each cell voltage. Error bars represent the standard deviation of the current density over three samples.

(B and C) Corresponding gas products (B) and liquid products (C) at each cell voltage. Error bars represent the standard deviation of three samples measured for each voltage.

(D) Full cell energy efficiency for all CO_2RR products and C_{2+} products at each cell voltage. Error bars represent the relative error from the standard deviation of the FE of three samples measured for each condition.

n-propanol, is likely due to diffusion and electroosmotic drag.[42] Although ethanol is a smaller molecule than n-propanol and would be expected to diffuse faster through the AEM to the anolyte, we offer that more ethanol remains on the cathode side of the electrolyzer because of its higher vapor pressure at room temperature. The full cell EE for C_{2+} products increased with increasing voltage despite the larger applied overpotentials due to the increase in C_{2+} FE (Figure S6B), reaching a maximum full cell C_{2+} EE of 20% (Figure 2D).

Flow Rate and Temperature Effects on MEA Performance

Maximizing product gas concentration is important to reduce the costs associated with the gas separation of dilute product streams. We pursued decreasing the CO_2 flow rate into the cell to evaluate the effect of CO_2 depletion along the gas channel. At each applied current density, we decreased the flow rate of CO_2 in increments from 40 to 2 sccm. The reaction favored a higher FE toward ethylene at lower CO_2 flow rates, reaching a peak ~50% FE at 2, 6, and 10 sccm of CO_2 (Figures 3A–3C) for the current densities of 50, 100, and 150 mA cm^{-2}, respectively. The increase in selectivity toward ethylene is attributed to a higher local pH at the catalyst layer due to the reduced reaction of CO_2 with hydroxide ions and a favorable CO_2*/CO* coverage on the Cu catalyst. Similar increases in ethylene selectivity were observed in the partial pressure experiments at low CO_2 concentrations (Figure S8). The selectivity toward ethanol reached a maximum of 20% FE at similar CO_2 flow rates as the maximum selectivity for ethylene (Figure S9). As the CO_2

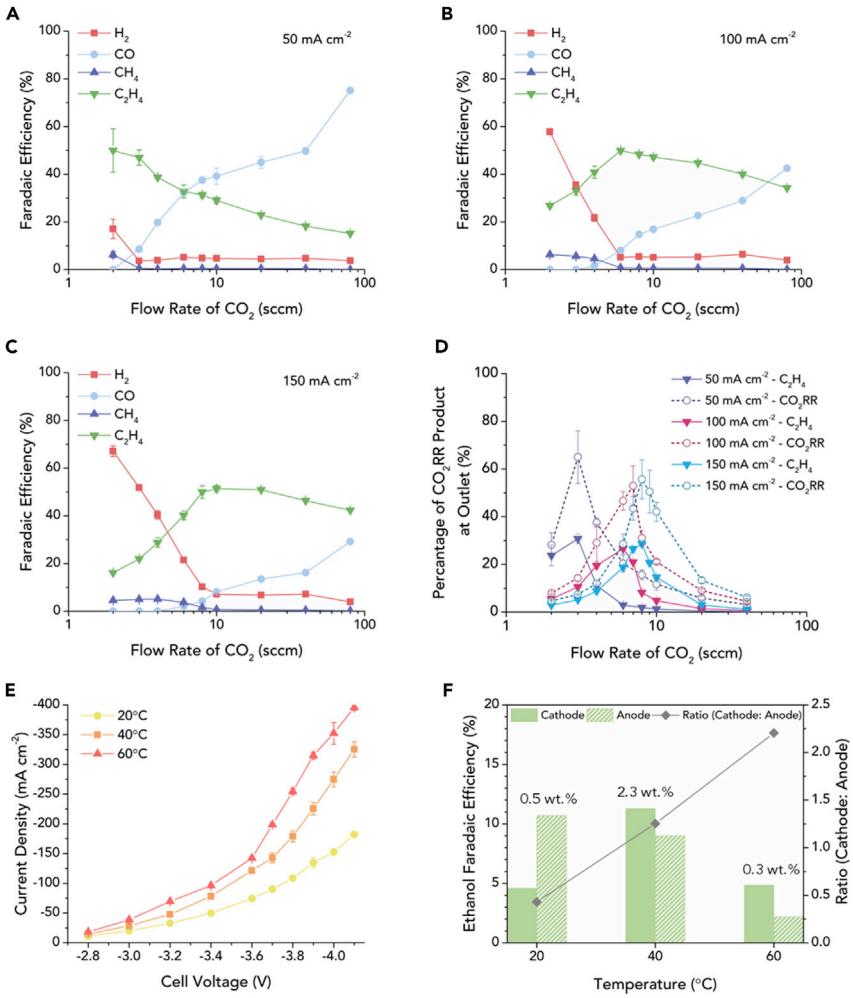

Figure 3. Increasing Gas and Liquid Product Concentrations at the Cathode Gas Outlet

(A–C) The effect of CO_2 flow rates on gas product selectivity at 50 mA cm^{-2} (A), 100 mA cm^{-2} (B), and 150 mA cm^{-2} (C). Error bars represent the standard deviation of three samples measured for each condition.

(D) Gas composition of cathode outlet gas as a percentage for ethylene and total CO_2RR product at 50, 100, and 150 mA cm^{-2}. Error bars represent the relative error from the standard deviation of the FE of three samples measured for each condition.

(E) Effect of temperature on the current density. Error bars represent the standard deviation of the current density over three samples.

(F) Amounts and ratios of ethanol FEs that are recovered from the cathode and anode streams at each temperature. The ethanol FEs were selected for the maximum cathode to anode ratio at each temperature.

flow rates were further reduced, the CO_2 single-pass conversion (defined as the ratio of CO_2 converted into CO_2RR products to the total CO_2 fed into the electrolyzer) continued to increase (>30% at 2 sccm) (Figure S9); however, when flow rates were reduced past the point of peak ethylene selectivity, we observed CO_2 mass transport limitations and, consequently, increased hydrogen production. The maximum concentration of the CO_2RR gas products in the gas outlet reached a peak of 65% at a flow rate of 3 sccm while operating at 50 mA cm^{-2}, with 30% of the outlet gas composed of ethylene (Figure 3D). This finding suggests that a system that depletes CO_2 along the channel could retain high FE performance toward CO_2RR and release concentrated gas products at the outlet.

Please cite this article in press as: Gabardo et al., Continuous Carbon Dioxide Electroreduction to Concentrated Multi-carbon Products Using a Membrane Electrode Assembly, Joule (2019), https://doi.org/10.1016/j.joule.2019.07.021

Next, we investigated the impact of temperature on the MEA performance and liquid product concentration. The current densities for the MEA system increased (Figure 3E) with temperature, a finding we assign to the increase in membrane ionic conductivity with temperature and improved reaction kinetics.[34] As a result, the partial current densities toward hydrogen (Figure S10A) and ethylene (Figure S10B) each increased with temperature, with a higher rate of increase for hydrogen. However, when considering the changes in kinetics of all the different reactions, it is observed that the peak ethylene FE decreased and shifted to less negative voltages (Figures S10C and S10E) with elevated temperatures. At higher temperature, we observed an increased recovery of generated ethanol at the cathode outlet compared to the amount that crossed to the anode (Figures 3F, S10D, and S10F), a finding we attribute to increased water transport from the anode to the cathode, and increased vaporization of ethanol from the higher temperatures. The maximum concentration of ethanol was achieved at 40°C and was measured to be 2.3 wt % (or 0.5 M), a significant enhancement in recovered product compared to the 0.5 wt % collected at 20°C.

Catalyst Tuning and MEA Stability

We hypothesized that the high availability of CO_2 in the MEA system would allow us to further tune the Cu catalyst toward maximal C_{2+} EE. Increasing the thickness of the Cu catalyst increases the active surface area for CO_2RR by taking advantage of the three-dimensional network of PTFE fibers in the GDL and allows for higher current densities. This catalyst modification is possible in an MEA based-system because of the elevated CO_2 concentration at the Cu catalyst compared to the alkaline flow cell (Figure S11). The alkaline flow cell has a short CO_2 diffusion length where a thin catalyst would be preferred to avoid HER[6]; however, the MEA is not as limited by CO_2 solubility, and reactant can diffuse further into the catalyst layer.

To develop a catalyst strategy for this MEA environment, we varied the thickness of the sputtered Cu to 50 and 250 nm, while screening the voltage to assess the activity of each catalyst (Figure 4A). Increasing the thickness of the sputtered Cu layer increases the coverage of the catalyst on the fibrous PTFE membrane support (SEM images of the catalysts of different thicknesses; Figures S1A, S11A, and S11B), accounting for increased electrical connection and decreased sheet resistance (Table S2). This increased interconnectivity of the catalyst also increases the available reaction area for CO_2RR. The 250 nm Cu catalyst reached peak ethylene at −3.9 V (Figure 4C) and achieved a high C_{2+} FE of ~80%, corresponding to an increase in the C_{2+} EE to 23% (Figure 4D). The ethanol that was recovered on the cathode when operating at room temperature reached ~2 wt % in the liquid cold trap (Figure 4F), a 4-fold increase in ethanol concentration compared to the 150 nm Cu catalyst also at 20°C.

By combining the optimized catalyst with higher temperatures, concentrated ethanol was generated which dissolved parts of the membrane and formed a hole within a couple hours of operation. Substituting the Sustainion X37-50 membrane with an Aemion AF1-CNN8-60-X membrane, we achieved 3.9 wt % (0.85 M) ethanol and 1.3 wt % (0.2 M) n-propanol on the cathode side while operating at 40°C with the 250 nm catalyst (schematic shown in Figure 4G). This represents the most concentrated alcohol production from CO_2RR reported to date. In addition, ethanol concentrations >1 wt % are required for energetically feasible distillation from aqueous solutions, with energy costs decreasing with increasing alcohol concentration.[10]

The stability of the MEA with the 250 nm Cu catalyst was evaluated through potentiostatic electrolysis at a cell voltage of −3.75 V. Gas products were collected

Please cite this article in press as: Gabardo et al., Continuous Carbon Dioxide Electroreduction to Concentrated Multi-carbon Products Using a Membrane Electrode Assembly, Joule (2019), https://doi.org/10.1016/j.joule.2019.07.021

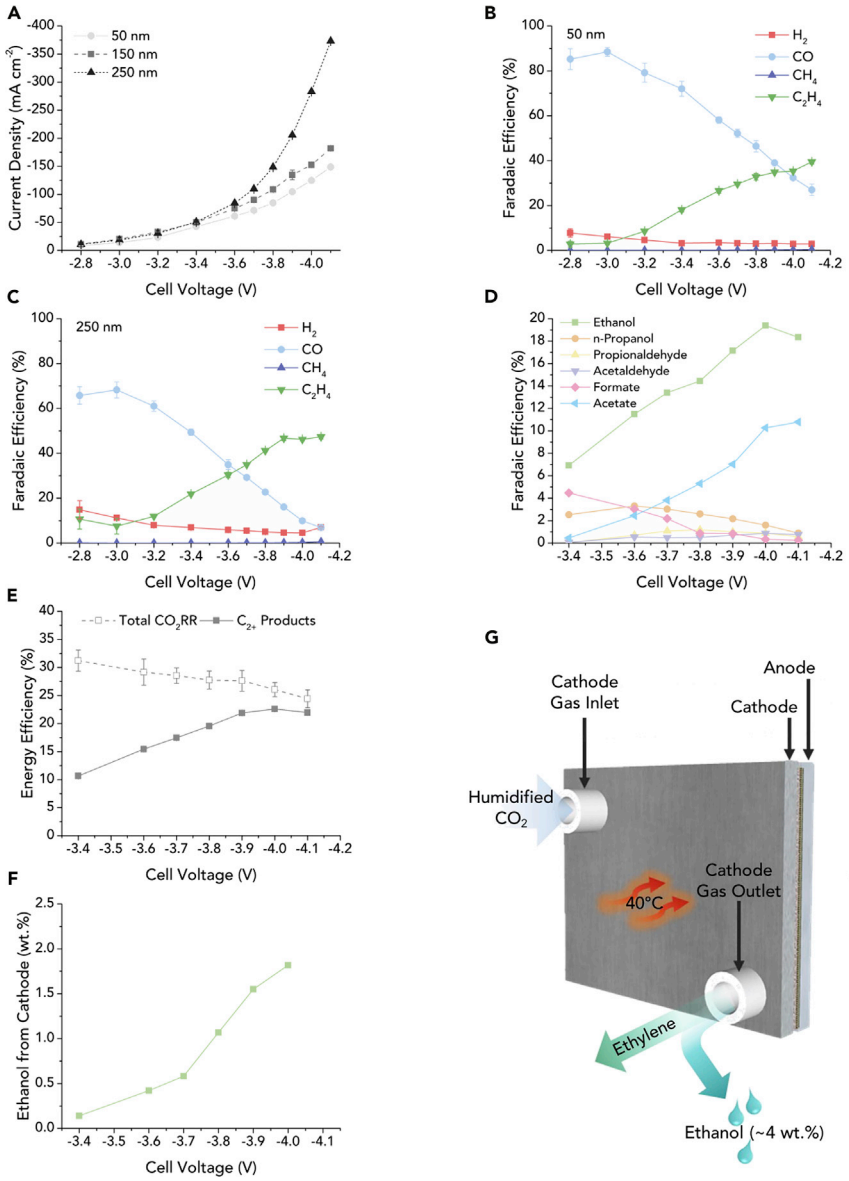

Figure 4. Catalyst Layer Optimization and Performance Characterization in an Mea Electrolyzer

(A) Relationship between current density and applied cell voltage for 50, 150, and 250 nm thick copper catalyst layers. Error bars represent the standard deviation of the current density over three samples.

(B and C) Gas product selectivity for 50 nm (B) and 250 nm (C) thick copper catalyst layers at each cell voltage. Error bars represent the standard deviation of three samples measured for each voltage.

(D) Liquid product selectivity from both the cathode and anode streams for the optimal 250 nm thick copper catalyst layer at each cell voltage.

(E) Energy efficiency for CO_2RR products and C_{2+} products at each cell voltage using the optimal 250 nm thick copper catalyst. Error bars represent the relative error from the standard deviation of the FE of three samples measured for each condition.

(F) Concentration of ethanol in the liquids collected from the cathode side for the 250 nm copper at each cell voltage.

(G) Schematic of the MEA electrolyzer for concentrated product generation.

Please cite this article in press as: Gabardo et al., Continuous Carbon Dioxide Electroreduction to Concentrated Multi-carbon Products Using a Membrane Electrode Assembly, Joule (2019), https://doi.org/10.1016/j.joule.2019.07.021

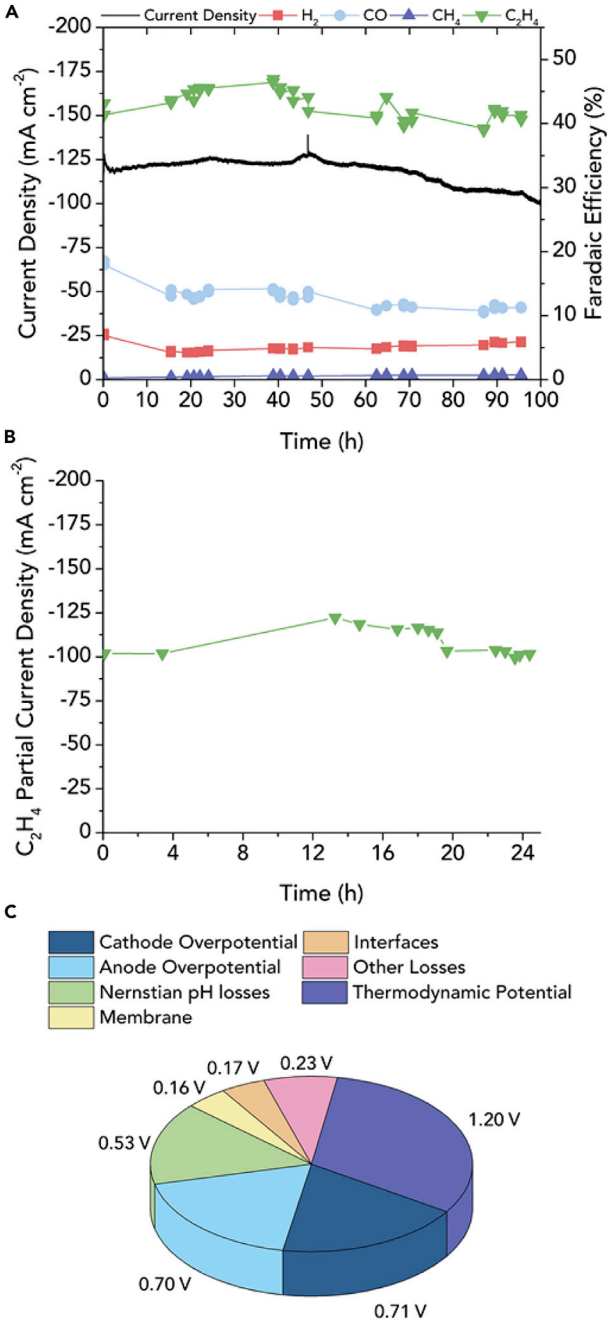

Figure 5. Long-Term Stability of the Mea Electrolyzer and Distribution of Voltage Losses

(A) Current density and gas products measured during 100 h of continuous operation at −3.75 V with the 250 nm thick copper catalyst.

(B) Stable ethylene partial current density for more than 24 h while operating at −3.9 V with the 250 nm thick copper catalyst. Total current density was >200 mA cm^{-2} at this applied cell voltage.

(C) Distribution of voltage losses measured in the MEA electrolyzer at 150 mA cm^{-2} (cell voltage of −3.7 V).

periodically and a single 200 mL volume of 0.1 M $KHCO_3$ anolyte was recirculated throughout the entire 100-h experiment. The MEA displayed a steady current density of approximately 120 mA cm^{-2}, as well as continuous ethylene production above 40% FE, throughout 100 h of operation (Figure 5A). Other gas products maintained

their FE across the experiment. In addition, the MEA electrolyzer used here is more similar to a commercial system with smaller electrolyte volume per area that is recirculated rather than refreshed, and a larger electrode area than previous C_{2+} electrolyzers.[6,7,13,43]

This duration of uninterrupted operation time is 2 orders of magnitude longer than in prior MEA electrolyzer reports of CO_2RR C_{2+} production. It is accomplished at one order of magnitude higher current density than in all prior MEA reports (Table S3). These improvements in ethylene stability were enabled by the combination of the robust Cu catalyst and PTFE GDE with the locally alkaline environment of the cathode. The MEA strategy was also assessed at a higher current density, >200 mA cm^{-2} by operating at a cell voltage of −3.9 V. The partial current density of ethylene was maintained >100 mA cm^{-2} throughout the entire 24 h operation (Figure 5B). Taken together, these results indicate that MEA systems enable increased stability in C_{2+} chemical production toward the ultimate target of commercially viable CO_2 electrolyzers.

The operating voltage of the MEA presented here is over 2 V higher than the thermodynamic potential of the cell based on the product distribution at 150 mA cm^{-2} (∼1.2 V). We performed an analysis to decouple all the sources of losses in our cell and highlight areas that could be reduced to further improve the system VE (Figure 5C). While operating at a current density of 150 mA cm^{-2}, we measured the cathode and anode overpotentials to be ∼0.71 and ∼0.70 V, respectively, accounting for the majority of the losses in the system. The overpotential at the cathode is similar to that of other C_{2+} alkaline liquid electrolyte flow cells,[7] however, the anode could be improved further. At the same current density, we determined the voltage loss at the membrane and interfaces to be ∼0.16 and ∼0.17 V, respectively, and the Nernstian pH losses to be ∼0.53 V. We have approximately ∼0.23 V of unassigned losses which can be attributed to errors in our determination of the other voltage loss sources in the system. We believe the accounting of the full MEA system losses presented here will help direct future efforts to decrease the energy demand of operating similar systems.

Conclusion

We developed a CO_2RR MEA electrolyzer strategy that outperforms incumbent liquid electrolyte flow cells in terms of voltage and product stability, as well as product concentration in the generation of C_{2+} products. The MEA electrolyzer operates at industrially relevant current densities while simultaneously achieving high selectivity toward multi-carbon products. The current densities reported here are at least an order of magnitude greater than other CO_2 to C_{2+} MEA electrolyzers.

Increasing operating temperature and decreasing CO_2 flow rate, enables concentrated output liquid and gas product streams, respectively. To take further advantage of the high CO_2 availability provided by the MEA, we designed a cathodic copper catalyst strategy to achieve a high FE and EE toward C_{2+} products (∼80% and 23%, respectively), while effectively shedding concentrated liquid products (3.9 wt % ethanol and 1.3 wt % n-propanol).

Finally, the stability of the MEA strategy was demonstrated through operation at industrially relevant current densities for 100 h while maintaining steady, high selectivity ethylene production. This is the only system, among all prior reactor reports, that has been reported to maintain current densities above 100 mA cm^{-2} for over 100 h with high and stable selectivity toward ethylene with continuously recirculated electrolyte.

Please cite this article in press as: Gabardo et al., Continuous Carbon Dioxide Electroreduction to Concentrated Multi-carbon Products Using a Membrane Electrode Assembly, Joule (2019), https://doi.org/10.1016/j.joule.2019.07.021

EXPERIMENTAL PROCEDURES

Electrode Preparation

Cathodes were prepared by sputtering 150 nm of Cu (99.99%) onto a porous PTFE membrane (0.45 μm pores), then airbrushed consecutively with carbon nanoparticle and graphite powder inks, as previously reported.[6] The anodes were prepared by depositing IrO_2 on a titanium support (0.002″ thickness, Fuel Cell Store) by a dip coating and thermal decomposition method.[32] Briefly, the titanium mesh was first degreased with acetone and DI water, then etched in a 6 M HCl (Reagent Grade, Bioshop) solution heated to 80°C to 90°C for 45 min before dip coating. The dip coating solution consisted of 30 mg of $IrCl_3 \cdot xH_2O$ (Alfa Aesar) dissolved in 10 mL of an isopropanol solution with 10% concentrated HCl. Subsequently, the etched titanium mesh was dipped into the $IrCl_3$ solution, dried in an oven at 100°C for 10 min before calcination in a furnace at 500°C for 10 min. The dipping and calcination process was repeated until a suitable loading was achieved (2 mg cm^{-2}).

Electrolyzer Configuration

The CO_2 reduction experiments in the MEA configuration were performed in a CO_2 electrolyzer cell (Dioxide Materials, grade 2 titanium anode, and 904L stainless steel cathode) with an active area of 5 cm^2 accessed with a serpentine channel. The experiments in the liquid flow cell configuration were performed in the same CO_2 electrolyzer with an additional 3 mm thick, laser cut PMMA catholyte flow chamber, sealed by two 1.5 mm silicone gaskets, resulting in a 6 mm electrode spacing (Figure S3). All the electrolyzer components were verified to be chemically resistant to all the reactants and products under the CO_2RR reaction potentials prior to experiments. An anion exchange membrane (Sustainion X37-50 Grade RT, Dioxide Materials, or Aemion AF1-CNN8-60-X, Ionomr) was inserted between the cathode and the IrO_2 coated titanium mesh. Throughout all experiments, unless otherwise specified, 80 sccm of humidified CO_2 was fed into the cathode flow channels using a mass flow controller (Sierra SmartTrak 100), while the anode side was fed with 0.1 M $KHCO_3$ electrolyte recirculated at 5 mL min^{-1} with a peristaltic pump. The cell was heated in the elevated temperature experiments using two heaters (Dioxide Materials), one on each side of the cell, connected to a temperature controller.

Electrochemical Measurements

An electrochemical workstation (Autolab PGSTAT204 with 10 A booster and FRA32 module) was used to measure the electrochemical response. The cell voltages reported in all figures were recorded without iR correction.

The analysis of the voltage losses in the MEA electrolyzer was conducted at 150 mA cm^{-2}. The cathode overpotential was measured using an Ag/AgCl reference electrode with 100% iR compensation in a flow cell with 0.5 M K_2CO_3 electrolyte. The anode overpotential was measured with an Ag/AgCl reference electrode with 100% iR compensation while in an H-cell with 0.1 M $KHCO_3$ electrolyte. In both cases, the iR compensation was calculated using the ohmic resistance determined through electrochemical impedance spectroscopy (EIS). The voltage losses in the membrane was determined as the difference in the full cell potential running with and without a membrane using 0.5 M K_2CO_3 electrolyte to ensure that the charge carrier through the membrane is the same as in the MEA cell, as determined by other modeling work[38] and supported with our COMSOL model. The voltage losses through interfaces in the MEA cell were calculated by subtracting the membrane losses from the full cell ohmic losses as determined using EIS between the anode and cathode of the MEA cell. The Nernstian pH losses were calculated from the difference in modeled local pH between the cathode and anode.

CO_2RR Product Analysis

The gas products from CO_2 reduction were taken from the cathode outlet in 1 mL volumes after at least 20 min of cell operation at a constant voltage or current to ensure stable performance. Flow rates and currents were measured just prior to collecting the gas sample. The gas samples were analyzed with a gas chromatograph (PerkinElmer Clarus 590) coupled with a thermal conductivity detector (TCD) and flame ionization detector (FID). The gas chromatograph was equipped with a Molecular Sieve 5A Capillary Column and a packed Carboxen-1000 Column with argon as the carrier gas. To determine the volume fraction of the gas products in our outlet, the peaks are integrated and compared to a calibration from known concentrations of a standard gas.

The liquid products were collected dripping from the gas side of the MEA using a cold trap (Supelco, Sigma Aldrich) cooled in a water bath at 0°C to also condense vapor-phase liquid CO_2RR products. The liquid products from the contents of the cold trap and the anolyte were quantified using proton nuclear magnetic resonance spectroscopy ($1H^+$ NMR) on an Agilent DD2 500 spectrometer in D_2O using water suppression mode, with dimethyl sulfoxide (DMSO) as the internal standard.

Calculations for FE and EE can be found in the Supplemental Information.

Electrode Characterization

The Cu catalyst surface and IrO_2 on Ti mesh were characterized using scanning electron microscopy (SEM) at Centre For Nanostructure Imaging at the University of Toronto using the Hitachi S-5200 high resolution scanning electron microscope.

COMSOL Continuum Transport Modeling

The system was modeled as a one-dimensional electrochemical cell for the reduction of CO_2 and H_2O in 0.1 M $KHCO_3$ with an AEM between the cathode and anode. The model assumed a constant supply of CO_2 into the catalyst layer from the GDE and a diffusion boundary layer thickness of 100 μm in the anolyte. The model made every attempt to mimic the experimental setup: the GDE was covered with a porous Cu catalyst layer, which was stabilized by carbon nanoparticles and graphite. The AEM separated the cathode and anode, after which anolyte was present. The species modeled include aqueous CO_2, CO_3^{2-}, HCO_{3-}, OH^-, H^+, K^+, and H_2O.

An in-depth model overview is outlined in previous literature,[44,45] but, briefly, we modeled all physics in COMSOL (COMSOL Multiphysics v5.4, Stockholm, Se) in one dimension. The model incorporated polarization losses (ohmic, diffusive, Nernstian), CO_2 solubility (pressure, temperature, and Sechenov effects), species transport (diffusive, reactive, and electromigrative), current density, and charge-transfer reactions at the cathode and anode toward CO_2RR, HER, and OER. The simulated charge-transfer reactions were matched to the experimentally observed rates. Feature conductivities and porosities were taken from empirical values. More details in the Supplemental Information.

SUPPLEMENTAL INFORMATION

Supplemental Information can be found online at https://doi.org/10.1016/j.joule.2019.07.021.

ACKNOWLEDGMENTS

The authors acknowledge support and infrastructure from the Natural Sciences and Engineering Research Council (NSERC), the Government of Ontario through the

Ontario Research Fund—Research Excellence program, and the Canada Foundation for Innovation. C.M.G. would like to thank NSERC for support in the form of a post-doctoral fellowship award. C.P.O. thanks the Province of Ontario for their funding toward graduate scholarships. J.P.E. thanks NSERC, Hatch, and the Government of Ontario for their support through graduate scholarships. Y.X. thanks NSERC for support in the form of a graduate scholarship. J.L. acknowledges the Banting Post-doctoral Fellowships program. D.S. acknowledges the NSERC E.W.R Steacie Memorial Fellowship and support from Canada Research Chairs Program. We would like to acknowledge CMC Microsystems for the provision of products and services that facilitated this research, including COMSOL Multiphysics.

AUTHOR CONTRIBUTIONS

C.M.G. and C.P.O. designed and carried out all experiments, as well as prepared the manuscript. J.P.E and Y.X. performed NMR analysis and aided with experimental setup. C.M. performed the COMSOL modeling simulations. C.T.D. and J.L. helped with discussion of experimental design. E.H.S. and D.S. supervised the project. All authors contributed to the discussion and analysis of data, as well as the editing of the manuscript.

DECLARATION OF INTERESTS

The authors declare no competing interests.

Received: April 29, 2019
Revised: May 22, 2019
Accepted: July 23, 2019
Published: August 21, 2019

REFERENCES

1. Whipple, D.T., and Kenis, P.J.A. (2010). Prospects of CO_2 utilization via direct heterogeneous electrochemical reduction. J. Phys. Chem. Lett. *1*, 3451–3458.

2. Bushuyev, O.S., De Luna, P., Dinh, C.T., Tao, L., Saur, G., van de Lagemaat, J., Kelley, S.O., and Sargent, E.H. (2018). What should we make with CO_2 and how can we make it? Joule *2*, 1–4.

3. Li, C.W., and Kanan, M.W. (2012). CO_2 reduction at low overpotential on Cu electrodes resulting from the reduction of thick Cu_2O films. J. Am. Chem. Soc. *134*, 7231–7234.

4. Raciti, D., Livi, K.J., and Wang, C. (2015). Highly dense Cu nanowires for low-overpotential CO_2 reduction. Nano Lett. *15*, 6829–6835.

5. Tang, W., Peterson, A.A., Varela, A.S., Jovanov, Z.P., Bech, L., Durand, W.J., Dahl, S., Nørskov, J.K., and Chorkendorff, I. (2012). The importance of surface morphology in controlling the selectivity of polycrystalline copper for CO_2 electroreduction. Phys. Chem. Chem. Phys. *14*, 76–81.

6. Dinh, C.T., Burdyny, T., Kibria, M.G., Seifitokaldani, A., Gabardo, C.M., García de Arquer, F.P.G., Kiani, A., Edwards, J.P., De Luna, P., Bushuyev, O.S., et al. (2018). CO_2 electroreduction to ethylene via hydroxide-mediated copper catalysis at an abrupt interface. Science *360*, 783–787.

7. Ma, S., Sadakiyo, M., Luo, R., Heima, M., Yamauchi, M., and Kenis, P.J.A. (2016). One-step electrosynthesis of ethylene and ethanol from CO_2 in an alkaline electrolyzer. J. Power Sources *301*, 219–228.

8. Jouny, M., Luc, W., and Jiao, F. (2018). General techno-economic analysis of CO_2 electrolysis systems. Ind. Eng. Chem. Res. *57*, 2165–2177.

9. Verma, S., Kim, B., Jhong, H.R.M., Ma, S., and Kenis, P.J.A. (2016). A gross-margin model for defining technoeconomic benchmarks in the electroreduction of CO_2. ChemSusChem *9*, 1972–1979.

10. Greenblatt, J.B., Miller, D.J., Ager, J.W., Houle, F.A., and Sharp, I.D. (2018). The technical and energetic challenges of separating (photo) electrochemical carbon dioxide reduction products. Joule *2*, 381–420.

11. Ripatti, D.S., Veltman, T.R., and Kanan, M.W. (2019). Carbon monoxide gas diffusion electrolysis that produces concentrated C_2 products with high single-pass conversion. Joule *3*, 240–256.

12. Díaz-Sainz, G., Alvarez-Guerra, M., Solla-Gullón, J., García-Cruz, L., Montiel, V., and Irabien, A. (2019). CO_2 electroreduction to formate: continuous single-pass operation in a filter-press reactor at high current densities using Bi gas diffusion electrodes. J. CO2 Util. *34*, 12–19.

13. De Luna, P., Quintero-Bermudez, R., Dinh, C.-T., Ross, M.B., Bushuyev, O.S., Todorović, P., Regier, T., Kelley, S.O., Yang, P., and Sargent, E.H. (2018). Catalyst electro-redeposition controls morphology and oxidation state for selective carbon dioxide reduction. Nat. Catal. *1*, 103–110.

14. Lv, J.J., Jouny, M., Luc, W., Zhu, W., Zhu, J.J., and Jiao, F. (2018). A highly porous copper electrocatalyst for carbon dioxide reduction. Adv. Mater. *30*, e1803111.

15. Kibria, M.G., Dinh, C.T., Seifitokaldani, A., De Luna, P., Burdyny, T., Quintero-Bermudez, R., Ross, M.B., Bushuyev, O.S., García de Arquer, F.P., Yang, P., et al. (2018). A surface reconstruction route to high productivity and selectivity in CO_2 electroreduction toward C_2+ hydrocarbons. Adv. Mater. *30*, e1804867.

16. Hoang, T.T.H.H., Verma, S., Ma, S., Fister, T.T., Timoshenko, J., Frenkel, A.I., Kenis, P.J.A.A., and Gewirth, A.A. (2018). Nanoporous copper-silver alloys by additive-controlled electrodeposition for the selective electroreduction of CO_2 to ethylene and ethanol. J. Am. Chem. Soc. *140*, 5791–5797.

17. Jouny, M., Luc, W., and Jiao, F. (2018). High-rate electroreduction of carbon monoxide to multi-carbon products. Nat. Catal. *1*, 748–755.

18. Pang, Y., Li, J., Wang, Z., Tan, C.-S., Hsieh, P.-L., Zhuang, T.-T., Liang, Z.-Q., Zou, C., Wang, X., De Luna, P., et al. (2019). Efficient electrocatalytic conversion of carbon monoxide to propanol using fragmented copper. Nat. Catal. *2*, 251–258.

19. Li, J., Che, F., Pang, Y., Zou, C., Howe, J.Y., Burdyny, T., Edwards, J.P., Wang, Y., Li, F., Wang, Z., et al. (2018). Copper adparticle enabled selective electrosynthesis of n-propanol. Nat. Commun. *9*, 4614.

20. Zhuang, T.-T., Pang, Y., Liang, Z.-Q., Wang, Z., Li, Y., Tan, C.-S., Li, J., Dinh, C.T., De Luna, P., Hsieh, P.-L., et al. (2018). Copper nanocavities confine intermediates for efficient electrosynthesis of C_3 alcohol fuels from carbon monoxide. Nat. Catal. *1*, 946–951.

21. Gabardo, C.M., Seifitokaldani, A., Edwards, J.P., Dinh, C.T., Burdyny, T., Kibria, M.G., O'Brien, C.P., Sargent, E.H., and Sinton, D. (2018). Combined high alkalinity and pressurization enable efficient CO_2 electroreduction to CO. Energy Environ. Sci. *11*, 2531–2539.

22. Jeanty, P., Scherer, C., Magori, E., Wiesner-Fleischer, K., Hinrichsen, O., and Fleischer, M. (2018). Upscaling and continuous operation of electrochemical CO_2 to CO conversion in aqueous solutions on silver gas diffusion electrodes. J. CO2 Util. *24*, 454–462.

23. Haas, T., Krause, R., Weber, R., Demler, M., and Schmid, G. (2018). Technical photosynthesis involving CO_2 electrolysis and fermentation. Nat. Catal. *1*, 32–39.

24. Kim, B., Ma, S., Molly Jhong, H.R., and Kenis, P.J.A. (2015). Influence of dilute feed and pH on electrochemical reduction of CO_2 to CO on Ag in a continuous flow electrolyzer. Electrochim. Acta *166*, 271–276.

25. Dufek, E.J., Lister, T.E., and McIlwain, M.E. (2012). Influence of electrolytes and membranes on cell operation for syn-gas production. Electrochem. Solid-State Lett. *15*, B48–B50.

26. Merino-Garcia, I., Albo, J., and Irabien, A. (2018). Tailoring gas-phase CO_2 electroreduction selectivity to hydrocarbons at Cu nanoparticles. Nanotechnology *29*, 014001.

27. Gutiérrez-Guerra, N., Valverde, J.L., Romero, A., Serrano-Ruiz, J.C., and de Lucas-Consuegra, A. (2017). Electrocatalytic conversion of CO_2 to added-value chemicals in a high-temperature proton-exchange membrane reactor. Electrochem. Commun. *81*, 128–131.

28. Aeshala, L.M., Uppaluri, R., and Verma, A. (2014). Electrochemical conversion of CO_2 to fuels: tuning of the reaction zone using suitable functional groups in a solid polymer electrolyte. Phys. Chem. Chem. Phys. *16*, 17588–17594.

29. Genovese, C., Ampelli, C., Perathoner, S., and Centi, G. (2013). Electrocatalytic conversion of CO_2 on carbon nanotube-based electrodes for producing solar fuels. J. Catal. *308*, 237–249.

30. Cook, R.L., Macduff, R.C., and Sammells, A.F. (1988). On the electrochemical reduction of carbon dioxide at in situ electrodeposited copper. J. Electrochem. Soc. *135*, 1320–1326.

31. Dewulf, D.W., and Bard, A.J. (1988). The electrochemical reduction of CO_2 to CH_4 and C_2H_4 at Cu/nafion electrodes (solid polymer electrolyte structures). Catal. Lett. *1*, 73–79.

32. Luc, W., Rosen, J., and Jiao, F. (2017). An Ir-based anode for a practical CO_2 electrolyzer. Catal. Today *288*, 79–84.

33. Zheng, T., Jiang, K., Ta, N., Hu, Y., Zeng, J., Liu, J., and Wang, H. (2019). Large-scale and highly selective CO_2 electrocatalytic reduction on nickel single-atom catalyst. Joule *3*, 265–278.

34. Kutz, R.B., Chen, Q., Yang, H., Sajjad, S.D., Liu, Z., and Masel, I.R. (2017). Sustainion imidazolium-functionalized polymers for carbon dioxide electrolysis. Energy Technol. *5*, 929–936.

35. Liu, Z., Masel, R.I., Chen, Q., Kutz, R., Yang, H., Lewinski, K., Kaplun, M., Luopa, S., and Lutz, D.R. (2016). Electrochemical generation of syngas from water and carbon dioxide at industrially important rates. J. CO2 Util. *15*, 50–56.

36. Hori, Y., Murata, A., and Yoshinami, Y. (1991). Adsorption of carbon monoxide, intermediately formed in electrochemical reduction of carbon dioxide, at a copper electrode. J. Chem. Soc. Faraday Trans. *87*, 125–128.

37. Peterson, A.A., Abild-Pedersen, F., Studt, F., Rossmeisl, J., and Nørskov, J.K. (2010). How copper catalyzes the electroreduction of carbon dioxide into hydrocarbon fuels. Energy Environ. Sci. *3*, 1311–1315.

38. Weng, L.-C., Bell, A.T., and Weber, A.Z. (2019). Towards membrane-electrode assembly systems for CO_2 reduction: a modeling study. Energy Environ. Sci. *12*, 1950–1968.

39. Burke, L.D., and O'Dwyer, K.J. (1989). Mediation of oxidation reactions at noble metal anodes by low levels of in situ generated hydroxy species. Electrochim. Acta *34*, 1659–1664.

40. Roca-Ayats, M., García, G., Soler-Vicedo, M., Pastor, E., Lázaro, M.J., and Martínez-Huerta, M.V. (2015). The role of Sn, Ru and Ir on the ethanol electrooxidation on Pt3M/TiCN electrocatalysts. Int. J. Hydr. Energy *40*, 14519–14528.

41. Hammond, C., Schümperli, M.T., Conrad, S., and Hermans, I. (2013). Hydrogen transfer processes mediated by supported iridium oxide nanoparticles. ChemCatChem *5*, 2983–2990.

42. Li, Y.C., Yan, Z., Hitt, J., Wycisk, R., Pintauro, P.N., and Mallouk, T.E. (2018). Bipolar membranes inhibit product crossover in CO_2 electrolysis cells. Adv. Sustainable Syst. *2*.

43. Hoang, T.T.H., Verma, S., Ma, S., Fister, T.T., Timoshenko, J., Frenkel, A.I., Kenis, P.J.A., and Gewirth, A.A. (2018). Nano porous copper-silver alloys by additive-controlled electrodeposition for the selective electroreduction of CO_2 to ethylene and ethanol. J. Am. Chem. Soc.

44. Singh, M.R., Clark, E.L., and Bell, A.T. (2015). Effects of electrolyte, catalyst, and membrane composition and operating conditions on the performance of solar-driven electrochemical reduction of carbon dioxide. Phys. Chem. Chem. Phys. *17*, 18924–18936.

45. Singh, M.R., Goodpaster, J.D., Weber, A.Z., Head-Gordon, M., and Bell, A.T. (2017). Mechanistic insights into electrochemical reduction of CO_2 over Ag using density functional theory and transport models. Proc. Natl. Acad. Sci. USA *114*, E8812–E8821.